Observation and Analysis of Multidomain Epitaxy of α-Mn on MgO(111)

Ilya L. Grigorov
Teledyne Electronic Technologies, Los Angeles, California 90066

M. R. Fitzsimmons
Manuel Lujan, Jr. Neutron Scattering Center, Los Alamos National Laboratory, Los Alamos, New Mexico 87545

I-Liang Siu and J. C. Walker
Department of Physics and Astronomy, The Johns Hopkins University, Baltimore, Maryland 21218
(Received 27 March 1998; revised manuscript received 10 December 1998)

Thin films of α-Mn were epitaxially grown on MgO(111) single-crystalline substrates at elevated temperatures in order to suppress the growth of metastable Mn phases previously reported. The α-Mn films were observed to have (110) texture, consistent with bcc (110) growth in Kurdjumov-Sachs orientation on the fcc (111) substrate surface, with additional twinning. The structural features observed for α-Mn(110) resemble those of metastable "expanded" Mn, indicating a possible connection between the two phases. [S0031-9007(99)09449-1]

PACS numbers: 68.55.Jk, 81.15.–z

Among transition metals, Mn has the most peculiar structural properties. The cubic unit cell of ground state α-Mn contains 58 atoms distributed over four special positions of the $I\bar{4}3m$ symmetry group. α-Mn is antiferromagnetic with $T_N = 95$ K [1]. Another low-temperature phase, β-Mn, has a simple cubic unit cell with 20 atoms and is paramagnetic. With increasing temperature, the unit cell of Mn becomes smaller, as two successive phase transitions, first to fcc and later to bcc phases, take place at 1095 and 1134 °C, respectively [2].

In previous studies, epitaxially grown thin films of Mn were shown to form phases which do not exist in the bulk. For example, the epitaxial growth of Mn on (001) cubic surfaces resulted in the formation of a tetragonal phase for a variety of substrate materials [3–5], although a relaxation of this phase to pseudomorphic fcc also has been reported [6]. The tetragonal phase was found to be antiferromagnetic at room temperature [4,5], an observation which is in good agreement with the theoretical predictions. These predictions suggest that the tetragonal distortion of fcc Mn is driven by magnetic ordering [7,8].

Deposited on the close-packed surfaces of fcc (111) and hcp (0001) substrates, Mn first assumes a close-packed structure with a lattice parameter close to that of fcc Mn [9]. This structure can persist up to thicknesses of 12 Å, depending on the temperature and composition of the substrate. Subsequently deposited Mn undergoes a $\sqrt{3} \times \sqrt{3}$ reconstruction to a so-called "expanded" phase [9–14]. Photoemission [10] and extended x-ray absorption fine structure [13] studies indicate that the electronic structure and interatomic distances in the expanded Mn phase are close to those of α-Mn. Several structural models of expanded Mn grown on close-packed surfaces have been proposed [9,12,14]. Some of these models [9,12] use the structure of α-Mn(111) as a prototype; however, the structure of the expanded phase is still unknown.

In this paper, we report a technique to epitaxially grow α-Mn directly on a close-packed surface without the formation of a metastable precursor Mn phase. Specifically, by using a MgO substrate with a large (11%) lattice parameter mismatch with respect to fcc Mn, and relatively high substrate temperature during deposition, the initial stabilization of the close-packed Mn, which tends to promote growth of the expanded phase at thicker coverages, was avoided. Previously, either the large lattice mismatch *or* the high deposition temperature resulted in growth of expanded Mn [10,14]. Further, the preferred texture of α-Mn on a surface with hexagonal symmetry is shown to be (110) rather than (111); the models interpreting the structure of expanded Mn in terms of α-Mn(111) structure should, therefore, be reexamined.

Mn was deposited on a mechanically polished MgO(111) substrate at a rate of 3–4 Å/min from a Knudsen cell heated to 880 °C. The base pressure in the deposition chamber was less than 2×10^{-10} Torr and did not exceed 8×10^{-10} Torr during sample growth. Before deposition, the substrate was annealed at 400 °C for two hours, producing a reflection high-energy electron diffraction (RHEED) pattern characteristic of MgO. The annealing temperature was chosen to be below 750 K (477 °C), the temperature required to cause (001) facets on the MgO (111) surface [15–17]. After annealing, the substrate temperature was lowered to 200 °C. The deposition of the first 8–10 Å of Mn was accompanied by the disappearance of the substrate RHEED pattern. Further deposition of Mn produced the sixfold symmetric RHEED pattern shown in Fig. 1. In addition to the bright streaks, a number of weak irregular reflections were observed. The deposition was stopped at a Mn thickness of 200 Å and the sample was cooled to room temperature in less than two hours. At this temperature, no discernible RHEED pattern could be observed.

The distances between the atomic rows on the Mn surface were calculated using the separation between the first order RHEED streaks (Fig. 1a). The rows parallel to the MgO $\langle 1\bar{1}0\rangle$ directions were spaced by 7.26 Å (Fig. 1a). In a direction perpendicular to MgO $\langle 1\bar{1}0\rangle$ the first order streaks appeared as doublets (Fig. 1b), indicating the presence of two sets of atomic rows spaced by 3.85 and 4.42 Å. The size of the Mn unit cell estimated from the product of the inter-row spacings in the MgO $\langle 1\bar{1}0\rangle$ and $\langle 11\bar{2}\rangle$ directions was quite large compared to the unit cell of the MgO substrate.

Further examination of the atomic structure of the Mn films was accomplished with *ex situ* x-ray diffraction at room temperature. The x-ray measurements were performed with a four-axis diffractometer at the Los Alamos Neutron Science Center using Cu $K\alpha$ radiation. Two kinds of measurements were made. The first was a conventional wide-angle diffraction scan used to determine the out-of-plane texture of the Mn layer. The second measurement used glancing incidence x-ray diffraction to determine the in-plane structure of the film. The angle of incidence was chosen to assure the whole thickness of the film was probed.

The wide-angle diffraction pattern taken from the Mn-MgO sample with momentum transfer parallel to the MgO [111] direction is shown in Fig. 2. The data are plotted versus scattering angle, 2Θ. Three Bragg reflections whose positions were consistent with the α-Mn crystal structure were observed, along with two reflections from the MgO substrate. The Mn reflections were indexed as ($hh0$), indicating the (110) texture of the film. A film with the (110) texture would exhibit twofold symmetry about the normal to the film, in contrast to the sixfold symmetry observed by RHEED (at 200 °C).

The 58-atom unit cell of α-Mn in the (110) orientation can be visualized as a sequence of eight planes. Each plane has the same surface lattice, with a unique atomic basis. The unit cell of this lattice is a centered rectangle, identical to an unit cell of the (110) plane of a simple bcc lattice with a lattice parameter $a = 8.91$ Å. Within the surface lattice, the distance between the atomic rows parallel to the $[1\bar{1}0]$ direction is 4.45 Å, while the distance between the rows parallel to the $[1\bar{1}1]$ direction is 7.27 Å.

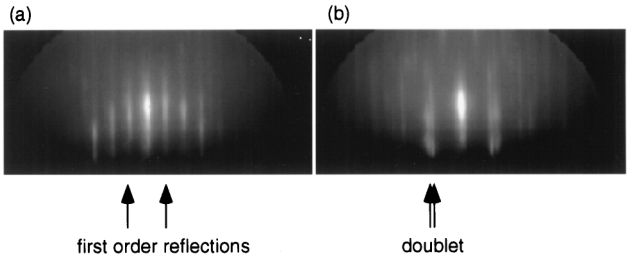

FIG. 1. Mn RHEED patterns obtained along (a) MgO $\langle 1\bar{1}0\rangle$ axes and (b) MgO $\langle 11\bar{2}\rangle$ axes. The absolute azimuthal angles are 0°, 60°, . . . , for (a); and 30°, 90°, . . . , for (b).

These values are consistent with the inter-row distances calculated from the RHEED pattern, provided α-Mn(110) grows on MgO(111) with the Mn [001] axis parallel to the MgO $\langle 1\bar{1}0\rangle$ axes. Three $\langle 1\bar{1}0\rangle$ axes on the MgO(111) surface will give rise to three degenerate Mn domains and a sixfold symmetric RHEED pattern with double streaks (Fig. 1b).

α-Mn growth on MgO(111) is reminiscent of the growth of bcc (110) overlayers on fcc (111) substrates extensively studied in a number of metallic multilayer structures [18–21]. This is perhaps surprising in light of the large and complex unit cell of α-Mn. However, some high-index planes of α-Mn parallel to the (110) plane contain only the atoms of the surface lattice (with no basis); therefore, the epitaxy of these planes on MgO(111) may be treated within the geometric approach developed for the analysis of the bcc-fcc epitaxy [22,23].

The (110) domains of a simple bcc overlayer usually grow on a fcc (111) substrate in two possible epitaxial orientations which correspond to the alignment of the different densely packed atomic rows of the overlayer and substrate. These orientations are the bcc [001] axis parallel to the fcc $\langle 1\bar{1}0\rangle$ axes, or the bcc $[1\bar{1}1]$ and $[\bar{1}11]$ axes parallel to the fcc $\langle 1\bar{1}0\rangle$ axes. The first case is called the Nishiyama-Wasserman (NW) orientation and gives rise to three rotationally related domains. The second case is called the Kurdjumov-Sachs (KS) orientation; six domains, in groups of two, are produced from this orientation. Recently, the third, Homma-Yang-Schuller (HYS), orientation has been observed with the domains rotated by 30° with respect to NW orientation [24]. The most favorable orientation, whether NW, HYS, or KS, is one that maximizes the commensuration between the surface lattices of the overlayer and the substrate in the direction perpendicular to the parallel rows of densely packed atoms [22,23]. The commensuration may be expressed in terms of the ratio, r, of the inter-row distances of the overlayer to the substrate. For perfectly

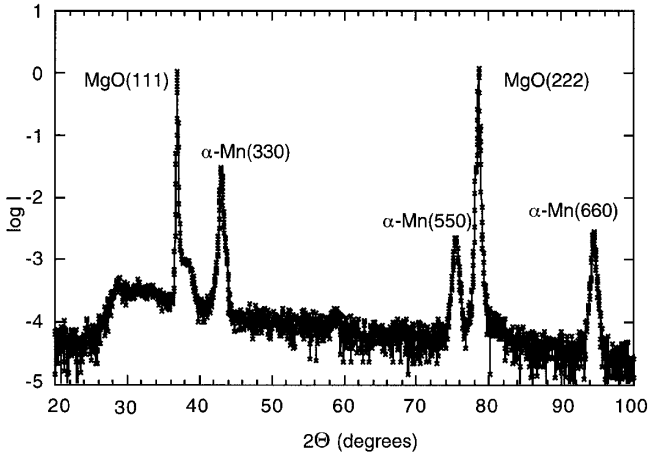

FIG. 2. Wide-angle x-ray diffraction spectrum. Momentum transfer is parallel to the MgO [111] direction.

commensurate structures r is an integer. The value of r calculated for the α-Mn(110)/MgO(111) system in the KS orientation is 2.82. In contrast, $r = 2.44$ and 1.73 for the NW and HYS orientations; thus the KS orientation is expected to be more energetically favorable than the others. For bcc Fe on Cu(111) $r = 1.06$ for the KS orientation, and $r = 0.92$ for the NW orientation. Although both values are close to unity, only the KS orientation was observed [20].

In order to elucidate the azimuthal orientation between the Mn overlayer and the substrate, glancing incidence x-ray diffraction [25] was performed on a sample with 200 Å of Mn on MgO to observe the in-plane crystallinity of the Mn layer. The intensity of the α-Mn $(3\bar{3}0)$ reflection was monitored as a function of the sample rotation, ϕ, about the surface normal. The intensity profile (Fig. 3) consists of 24 peaks with the same width (full width at half maximum $\approx 2.7°$) in groups of four. Since the $(3\bar{3}0)$ reflection is twofold symmetric, the occurrence of these peaks suggests the presence of *twelve* rather than three or six domains.

The positions of two inner peaks in each group are displaced by $\pm 5.25°$ from center of the group (see the inset of Fig. 3) which coincides with the $\langle 11\bar{2}\rangle$ direction of MgO. Since the latter direction is parallel to an α-Mn $(3\bar{3}0)$ reciprocal lattice vector in the NW orientation, and no peak was observed at this location, α-Mn does not assume the NW orientation. The absence of diffraction peaks rotated by $\pm 30°$ with respect to the NW orientation eliminates the presence of HYS domains. Rather, the splitting of the inner peaks is consistent with the KS orientation, and in agreement with the commensuration arguments discussed earlier.

The outer peaks of the quadruplet, displaced by $\pm 15.2°$ from center, can be produced by twinning of the KS domains. The primitive surface unit cell of any bcc structure in the (110) orientation is a rhombus with 70.6° and 109.4° angles. If a $(1\bar{1}2)$ twin plane is formed, the crystallites on the opposite sides of the plane will be rotated by a twinning angle of 70.6° with respect to each other. An example of such a twin is shown in Fig. 4a. The angle of rotation is in good agreement (considering the linewidth) with the angle ($\approx 70.2°$) measured between the inner line of one quadruplet and one of the outer lines of the adjacent quadruplet (Fig. 4b). Each crystallite has two potential twin boundaries [along $(1\bar{1}2)$ and $(1\bar{1}\bar{2})$ planes]; therefore, given the presence of the six original KS domains, 12 more domains are produced from twinning, for a total of 18. While formation of one twin boundary produces the domain with a new orientation [domain (2), Fig. 4a], the other twin is aligned with one of the original KS domains [domain (3), Fig. 4a]. The number of the domains with

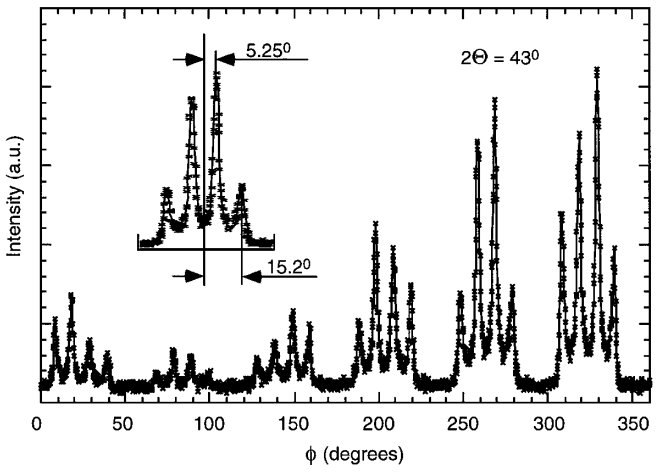

FIG. 3. The α-Mn $(3\bar{3}0)$ reflection observed as a function of rotation angle, ϕ, about the surface normal of the sample.

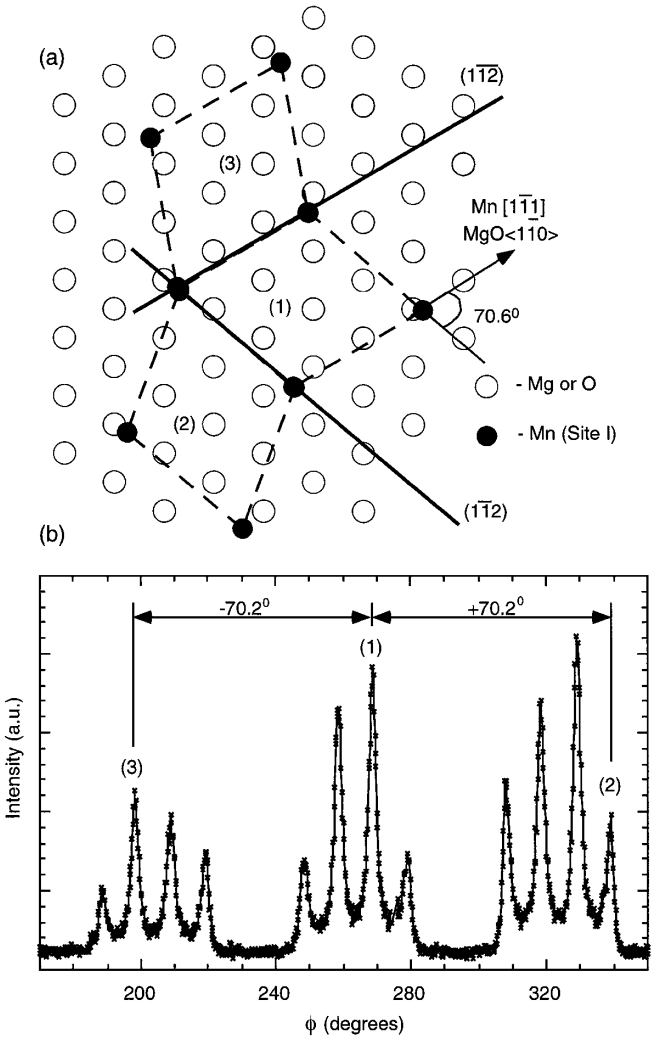

FIG. 4. (a) Twinned domains of α-Mn(110) on MgO(111) surface. Domain (1) is in the KS orientation, domain (2) is a "misaligned" twin, and domain (3) is an "aligned" twin. Twins are rotated by $\pm 70.6°$ with respect to domain (1). Solid lines represent the projections of the twin boundaries onto the Mn(110) plane. (b) The correspondence between the angular separation of diffraction lines and rotations of twinned domains.

the unique orientations is reduced to 12, producing the 24 peaks observed in the diffraction pattern.

Since the surface lattice of the "misaligned" twin [domain (2), Fig. 4a] is not commensurate to the MgO surface, as neither of the densely packed atomic rows of two crystals are parallel, these crystallites are not likely to have been nucleated during the initial stages of the film growth. Rather, they are likely to have formed on the facets of the KS domains due to defects such as stacking faults, or as a mechanism to accommodate strain in the Mn film. The limited mobility of the Mn atoms on the surface at 200 °C may help stabilize the faults [26]. The average ratio of the line intensities of the Bragg reflections from the incommensurate twins to those of the commensurate domains (KS and "aligned twins") is 0.46 (8). From this number, the fraction of the Mn layer consisting of misaligned twins is calculated to be roughly one-third. A film with such a large fraction of twinned material present during deposition should have produced a RHEED pattern with the symmetry similar to that of the x-ray rotational scan (Fig. 3) rather than the observed sixfold symmetry. The noted disappearance of the RHEED streaks, and an increased diffuse scattering after the sample cooled to room temperature, are indicative of changes in the sample surface morphology, such as increased surface roughness. Such changes may be a consequence of the formation of twins in the film bulk (establishing an unambiguous correlation between these two phenomena requires techniques not available in this study). Hence, the formation of the twins occurred while the sample was cooling from 200 °C, the temperature at which a well-defined RHEED pattern was observed, to room temperature.

Given the opportunity to form the stable α-Mn phase on a close-packed surface, Mn grows with the (110) texture, suggesting that this structure is more plausible as a prototype for the atomic arrangement of metastable expanded Mn than α-Mn in the (111) orientation. The experimental data seem to support this conjecture: An in-plane x-ray diffraction pattern of the expanded Mn films grown on Ag(111) and Cu(111) matches that of α-Mn(110) in the NW orientation with an additional expansion of the in-plane lattice parameter by 5% [14].

In summary, the structure of a Mn film on MgO(111) grown under conditions favoring the growth of the thermodynamically stable α-Mn phase was studied. The formation of multidomain α-Mn in the (110) orientation was observed. The domain structure can be explained by a combination of nucleated crystallites with the KS orientation and twin formation. As some of the twins are not commensurate to the substrate, their formation is likely driven by grain boundary imperfections, perhaps as a mechanism to relieve stress in the film. The growth features of α-Mn in the (110) plane can be understood in terms of the surface unit cell alone, without considering the complex atomic basis. Finally, the demonstrated epitaxial growth of thin film α-Mn should motivate studies of magnetic compensation in various crystal planes of this metal by means of the exchange bias in a bilayer comprised of α-Mn and a ferromagnetic overlayer [14].

Portions of this study were supported by NSF Grant No. 9410148 and the U.S. Department of Energy BES-DMS under Contract No. W-7405-Eng-36. We thank Dr. M. Hawley, Dr. G. Brown, and Dr. J. Larese for useful discussions, and Dr. Q. Jia for additional financial support.

[1] J. S. Kasper and B. W. Roberts, Phys. Rev. **101**, 537 (1956).
[2] W. B. Pearson, *A Handbook of Lattice Spacings and Structures of Metals and Alloys* (Pergamon, New York, 1958).
[3] D. Tian, S. C. Wu, F. Jona, and P. M. Marcus, Solid State Commun. **70**, 199 (1989).
[4] B. T. Jonker, J. J. Krebs, and G. A. Prinz, Phys. Rev. B **39**, 1399 (1989).
[5] T. G. Walker and H. Hopster, Phys. Rev. B **48**, 3563 (1993).
[6] P. Schieffer *et al.,* J. Magn. Magn. Mater. **165**, 180 (1997).
[7] T. Oguchi and A. J. Freeman, J. Magn. Magn. Mater. **46**, L1 (1984).
[8] P. Krüger *et al.,* J. Magn. Magn. Mater. **156**, 91 (1996).
[9] A. S. Arrott *et al.,* J. Appl. Phys. **61**, 3721 (1987).
[10] D. Tian *et al.,* Phys. Rev. B **45**, 3749 (1992); D. Tian, A. M. Begley, and F. Jona, Surf. Sci. Lett. **273**, L393 (1992).
[11] V. L. O'Brien and B. P. Tonner, J. Vac. Sci. Technol. A **13**, 1544 (1995).
[12] K. Ounadjela *et al.,* Phys. Rev. B **49**, 8561 (1994).
[13] S. Andrieu *et al.,* Phys. Rev. B **54**, 2822 (1996).
[14] I. L. Grigorov and J. C. Walker, J. Appl. Phys. **81**, 3907 (1997); I. L. Grigorov *et al.,* J. Appl. Phys. **83**, 7010 (1998)
[15] Victor E. Henrich, Surf. Sci. **57**, 385 (1976).
[16] H. Onishi *et al.,* Surf. Sci. **191**, 479 (1987).
[17] C. R. Henry and H. Poppa, Thin Solid Films **189**, 303 (1990).
[18] H. L. Gaiger and N. G. van der Berg, Thin Solid Films **146**, 299 (1987).
[19] Y. Ando and D. J. Dingley, J. Cryst. Growth **99**, 601 (1990).
[20] D. Tian, F. Jona, and P. M. Marcus, Phys. Rev. B **45**, 11 216 (1992).
[21] A. M. Begley *et al.,* Surf. Sci. **280**, 289 (1993).
[22] E. Bauer and Jan H. van der Merwe, Phys. Rev. B **33**, 3657 (1986).
[23] Akiko Kobayashi and S. Das Sarma, Phys. Rev. B **35**, 8042 (1987).
[24] Sun M. Paik and Ivan K. Schuller, Phys. Rev. Lett. **64**, 1923 (1990); H. Homma, Kai-Y. Yang, and I. K. Schuller, Phys. Rev. B **36**, 9435 (1987).
[25] H. Dosch, Phys. Rev. B **35**, 2137 (1987).
[26] D. J. Godbey and M. E. Twigg, J. Appl. Phys. **69**, 4216 (1991).